

NUMERICAL STUDY OF FLAME STRUCTURE IN THE MILD COMBUSTION REGIME

by

Amir MARDANI^{a*} and Sadegh TAJEMAAAT^b

^a Department of Aerospace Engineering, Sharif University of Technology, Tehran, Iran

^b Department of Aerospace Engineering, Amirkabir University of Technology, Tehran, Iran

Original scientific paper

DOI: 10.2298/TSCI120522091M

In this paper, turbulent non-premixed $CH_4 + H_2$ jet flame issuing into a hot and diluted co-flow air is studied numerically. This flame is under condition of the moderate or intense low-oxygen dilution combustion regime and related to published experimental data. The modelling is carried out using the EDC model to describe turbulence-chemistry interaction. The DRM-22 reduced mechanism and the GRI2.11 full mechanism are used to represent the chemical reactions of H_2 /methane jet flame. The flame structure for various O_2 levels and jet Reynolds numbers are investigated. The results show that the flame entrainment increases by a decrease in O_2 concentration at air side or jet Reynolds number. Local extinction is seen in the upstream and close to the fuel injection nozzle at the shear layer. It leads to the higher flame entrainment in the moderate or intense low-oxygen dilution regime. The turbulence kinetic energy decay at centre line of jet decreases by an increase in O_2 concentration at hot co-flow. Also, increase in jet Reynolds or O_2 level increases the mixing rate and rate of reactions.

Key words: moderate or intense low-oxygen dilution combustion, dilution, flame structure, turbulent non-premixed combustion, preheat

Introduction

The moderate or intense low-oxygen dilution (MILD) combustion is acronym of moderate or intense low-oxygen dilution combustion [1]. It is a process in which, the reactants mixture temperature in the reaction zone is higher than the self-ignition temperature of the mixture and maximum temperature increase during combustion is lower than self-ignition temperature of the reactant mixture. MILD combustion, high temperature air combustion (HiTAC) [1-3], high temperature combustion technology (HiCOT) [1, 4], and flameless combustion [1, 5] are broadly similar technologies. In the past two decades, many investigations have been carried out on combustion under MILD condition. They showed that higher reaction zone volume [6, 7], lower temperature gradient, lower combustion noise [5], smaller temperature oscillations in the reaction zone [3, 5] and sometimes colourless oxidation of fuel [8, 9] occur under such conditions (*i. e.* high temperature preheating and dilution) with respect to ordinary combustion processes. Lower emission production and fuel consumption are substantial benefits of this combustion regime [10-12]. For instance, Hasegawa *et al.* [13] reported that pollutant emission (like

* Corresponding author; e-mail: amardani@sina.sharif.edu

nitric oxides) decreases up to 50%, fuel consumption decreases up to 30% and furnaces down-sizes up to 25% under HiTAC condition. Also, the MILD combustion demonstrates lower reaction rate, lower heat release rate, and lower Damkohler number (Da) in comparison with the ordinary combustion regime [3, 14].

In a MILD combustion regime, the reduction in the rate of heat release and oxygen concentration provides a condition quite different from that of an ordinary combustion. Therefore, damping of turbulence eddies and re-laminarization are done in different levels in comparison to ordinary combustion processes. Mortberg *et al.* [15] studied the flow dynamic of normal and low calorific fuels in HiTAC condition using cross-flow jet arrangement. They reported a slower mixing, higher turbulence and higher axial strain rate for low calorific fuel jets as compared to methane fuel under the HiTAC condition. Christo *et al.* [16] studied the turbulent non-premixed CH₄/H₂ jet flames issuing into a heated and highly preheated co-flow. They reported that the molecular transport has a strong effect on the MILD combustion regime. Kim *et al.* [17] applied the conditional moment closure (CMC) model to the experimental conditions of Dally *et al.* [18], which are at MILD conditions. A non-negligible effect of the differential diffusion on the MILD combustion was confirmed by them, too. Also, the importance of molecular diffusion in MILD combustion is studied comprehensively in other paper of authors [19]. Turbulent non-premixed jet flame under the condition of HiTAC was investigated by Kobayashi *et al.* [20]. They showed that the turbulence decay is not large under HiTAC. The entrainment of a turbulent jet in co-flow under HiTAC has been studied numerically by Yang *et al.* [21] and Oldenhof *et al.* [22], separately. They reported that the entrainment increases under the more uniform the heat release. Medwell *et al.* [23] reported measurements in a co-flow jet flame under the MILD combustion regime. The spatial distribution of OH, H₂CO and temperature were compared between three jet Reynolds numbers and two O₂ levels. Parente *et al.* [24] presented a numerical and experimental investigation of a burner operating in the MILD combustion regime with methane and methane-hydrogen mixtures. They concluded that the effects of molecular diffusion on the temperature field and on the major species are negligible for their MILD combustion system. This is in contrast to the behaviour observed by Christo *et al.* [16] and the results of authors [19], which Parente attributes to the intense re-circulation.

Gupta [25] has predicted the application of HiTAC combustion technology in several industries like micro GT, thermal destruction, fuel cell, *etc.*, although this technology has been successfully developed in industrial furnaces and also is in progress in some other industries like boilers and steam reformers. Some of these implementations are performed with little understanding about the detail structure of the MILD regime. But for further development of this new technology, there is still a desperate need for more investigations on detail structure of the MILD combustion regime. Only a few fundamental studies have been performed on this subject (*e. g.*, [1, 18, 22, 23]). It can be inferred from the above literature that most papers on MILD combustion are more focused on targets different from the fluid dynamics itself and this field can be still studied in more detail. This idea was mentioned by several review contributions [1, 26, 27]. Furthermore few coherent experimental data has led to fewer numerical comprehensive studies of flame structure of the MILD combustion. Sensitivity studies of flame structure parameters (like entrainment of fuel jet or velocity profile or mixture fraction distribution or minor species distribution) to MILD combustion characteristics, like O₂ concentration level and fuel jet Reynolds number, could be accurately explored by numerical modelling. The fuel jet emerging into a very lean and hot atmosphere can emulate MILD combustion under controlled conditions. Such conditions (*i. e.* hot and very lean atmosphere as high as 1300 K and 3% oxygen, respectively) are less considered in most of the research into non-premixed jet flames. Also at

some interesting reports on flame structure of MILD combustion such as Yang *et al.* [21], a two-step mechanism is used and the comparison of numerical and experimental results is not so extensive.

Following the previous works of Mardani *et al.* [19, 28-30], this study focuses on studying the flame structure and effect of fluid dynamics on MILD combustion characteristics. In this way, we used computational fluid dynamic modelling of a turbulent non-premixed CH_4/H_2 jet flames issuing into a heated and highly preheated co-flow. The numerical modelling is done for cases measured by Dally *et al.* [18]. The effects of O_2 concentration, in hot co-flow airside, and jet Reynolds number on the flame structure are investigated. In particular, the fluid dynamics and mixing are studied by focusing on the reaction zone characteristics, flame entrainment, Damkohler number distribution, turbulence kinetic energy decaying, and so on.

Numerical modeling description

The experimental burner geometry of Dally *et al.* [18] is used for numerical modelling in this study. The fuel is a H_2/CH_4 jet in a hot co-flow (JHC) mounted in a wind tunnel. In the tunnel, air flows at 3.2 m/s parallel to the burner axis, and the flame can be assumed axisymmetric. The equivalent axisymmetric constructed computational domain is shown in fig. 1.

The governing equations consist of axisymmetric incompressible Favre-averaged form of Navier-Stokes [31] and modified standard $k-\varepsilon$ equations [16]. The resulting equations are solved by an in-house FORTRAN code. The flow solver is written for the modelling reactive flows containing detailed chemistry in 2-D and axisymmetric geometries. It is based upon the Patankar SIMPLER algorithm using the control-volume method constructed on a non-staggered orthogonal grid [32]. The quadratic upstream interpolation for convective kinetics (QUICK) scheme of Leonard (1979) is used for discretizing the equations. It uses a three-point upstream weighted quadratic interpolation for cell face values.

Boundary conditions at the upstream are set by velocity profiles and inlet temperature and species mass fractions and the other boundary conditions are according to fig. 1. The velocity profiles at the inlets are estimated from non-reacting flow field modeling inside the burner. The results of the present research illustrate that the solution is not sensitive to turbulence intensity at the hot co-flow and wind tunnel inlets, which is also reported by [16, 33]. However, the turbulence intensity at the fuel inlet is important. Dally *et al.* [18] did not report the experimental data relating to the turbulence. However, Christo *et al.* [16] reported that the experimentally estimated mean turbulent kinetic energy of $16 \text{ m}^2/\text{s}^2$ (approximately equivalent to turbulence intensity of 4%) at the fuel inlet has been adjusted to $60 \text{ m}^2/\text{s}^2$ in their modelling (corresponding to turbulence intensity of 7.5%). In the present study, the fuel turbulence intensity adjusted to 7% to yield the best agreement between the calculated and measured mixture fraction distribution.

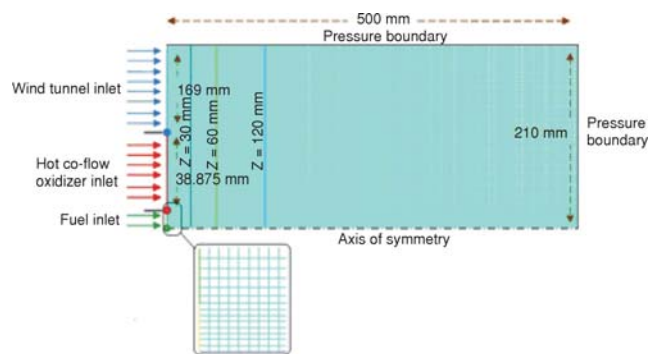


Figure 1. Numerical model geometry (it is not to scale but the zoomed area is to scale)

Three criteria are chosen for identifying the solution convergence. The first is to ensure that the residuals of all variables drop below 10^{-4} while a threshold of 10^{-6} was used for the temperature residual. The second is to ensure that the residuals of all variables are stabilized and are no longer changing with iterations. The third is to ensure that the maximum temperature fluctuation, with iterations, at the location of peak temperature drops below 0.1 K at three distances of 30, 60, and 120 mm from the nozzle.

Coupling the turbulence and chemistry is addressed by focusing on MILD combustion features and the other research reports. The characteristics of MILD combustion regime, such as low reaction rates and comparable reaction and turbulence time scales [3, 14, 16, 34], let us assume the reaction zone as a well-stirred reactor (WSR) [17]. The characteristic of the WSR entails the high level mixing (*i. e.* the more homogeneous mixture) and also a long average residence time inside the reactor (*i. e.* finite rate reactions). From this point of view, it is possible to find some similarities between characteristics of the EDC model and the WSR qualitatively. Therefore, the eddy-dissipation-concept (EDC) [35] model, which is an extension of the eddy-dissipation model to include detailed chemical mechanisms in turbulent flows, can be suitable for coupling the turbulence and chemistry. The EDC model assumes that reaction takes place in the small turbulent structures, namely the fine scales [35]. The volume fraction of the fine scales is modelled using the flow field turbulence characteristics, in which each structure is a constant-pressure-reactor (CPR), under conditions of homogeneous, Arrhenius finite rate law and detail chemical mechanisms over a special residence time. The EDC model is also introduced as a suitable model for MILD combustion in some other reports [16, 36]. Also, using the EDC model in MILD combustion modeling led to good results in previous papers of Mardani *et al.* [19, 28]. Moreover, using the EDC model in MILD combustion modeling is studied compressively by De *et al.* [37].

According to the results of Christo *et al.* [16] which is related to the JHC configuration, thermal radiation was ignored in this research.

DRM-19 and DRM-22 kinetic mechanisms [38] are reduced versions of the GRI1.2 [39]. They consist of 19 and 22 species, plus Ar and N₂, for a total 84 and 104 reversible reactions, respectively. A comparison between the results of the DRM-19 and GRI3.0 for the modeling of MILD combustion has been given by Kim *et al.* [17]. They reported good agreement between the results of these two kinetic mechanisms. Kazakov *et al.* [38] showed better performance of the DRM-22 than the DRM-19 in predicting ignition delay and laminar flame speed in atmospheric pressure. Therefore, the DRM-22 is used as a reduced kinetic mechanism in this study. In the present work, the GRI2.11 [40] is also used as a full kinetic mechanism. It consists of 49 species for a total 279 reversible reactions.

The strain rate is a useful parameter for studying the flame aerodynamic. The mixing rate could be characterized by the scalar dissipation rate, which is related to the strain rate [41]. Therefore, the strain rate could provide a measure of the mixing rate. The strain rate is defined as [31]:

$$S = \sqrt{\frac{\partial u}{\partial z} \left(\frac{\partial u}{\partial z} + \frac{\partial u}{\partial z} \right) + \frac{\partial u}{\partial r} \left(\frac{\partial u}{\partial r} + \frac{\partial v}{\partial z} \right) + \frac{\partial v}{\partial z} \left(\frac{\partial v}{\partial z} + \frac{\partial u}{\partial r} \right) + \frac{\partial v}{\partial r} \left(\frac{\partial v}{\partial r} + \frac{\partial v}{\partial r} \right)} \quad (1)$$

In this study, the flame entrainment is defined according to definition of Yang *et al.*, [21]. It is the ratio of the mass flow rate through the cross-section of the flame (m_e) to the initial jet mass flow rate (m_o) as follows:

$$R_{\text{ent}} = \frac{m_e}{m_o} \quad (2)$$

In the research of Yang, the flame volume is indicated by an approximation way, which is verified in their other reports [42, 43]. In this paper, the flame boundaries and the cross-section of the flame are identified by the position corresponding to maximum OH mass fraction.

For further detail, the Damkohler number is also calculated. The Damkohler number is the turbulence-to-chemical time scales, and it changes for different turbulence time scales. In the present study, the turbulent Damkohler numbers is defined for the smallest eddies (Kolmogorov) as:

$$\text{Turbulence Damkohler number } ([31]) \equiv Da_T \equiv \sqrt{\frac{\nu c_r^2}{\varepsilon}} \quad (3)$$

$$\text{The chemical - reaction rate constant } \equiv c_r = \frac{\max_{1 < i < 104} \text{Arthenius rate of reaction No. } i}{\rho} \quad (4)$$

where ν is the kinematic viscosity, ε – the local dissipation rate of turbulent kinetic energy, ρ – the local mixture density, and c_r – the local parameter which defined as the maximum of chemical reaction rate constant among 104 reactions of DRM-22 chemical mechanism.

Results and discussion

The flame structure of the MILD combustion was calculated for seven cases. In these cases, fuel is mixture of 20% H₂ and 80% CH₄ on mass-basis. The wind tunnel air consists of 23% O₂ and 77% N₂ (mass basis). The mean inlet velocity of hot co-flow is set to 3.2 m/s same as wind tunnel air velocity. The mean fuel mixture jet, hot co-flow, and wind tunnel air temperature are 305, 1300, and 300 K, respectively. The specifications of these cases are given in tab. 1.

Table 1. Specifications of numerical experiments of this research (mixture composition fractions are in mass basis style)

No.	Jet Reynolds number	Hot oxidizer composition	Chemical mechanism
1	10000	9% O ₂ + 6.5% H ₂ O + 5.5% CO ₂ + 79% N ₂	GRI2.11
2	10000	3% O ₂ + 6.5% H ₂ O + 5.5% CO ₂ + 85% N ₂	GRI2.11
3	10000	9% O ₂ + 6.5% H ₂ O + 5.5% CO ₂ + 79% N ₂	DRM-22
4	10000	3% O ₂ + 6.5% H ₂ O + 5.5% CO ₂ + 85% N ₂	DRM-22
5	10000	23% O ₂ + 6.5% H ₂ O + 5.5% CO ₂ + 65% N ₂	DRM-22
6	5000	9% O ₂ + 6.5% H ₂ O + 5.5% CO ₂ + 79% N ₂	DRM-22
7	5000	3% O ₂ + 6.5% H ₂ O + 5.5% CO ₂ + 85% N ₂	DRM-22

As shown in fig. 1, the computational domain starts at the exit plane of the burner. It is axisymmetric model that extends 500 mm in axial direction and 210 mm in radial direction from the jet axis. At first, a grid study was done and a structural grid with 39000 cells was selected for calculations. It is a non-uniform grid with higher resolution in the upstream and close to the inlets and axis. The grid independency of results was verified using finer grids and ensured that the grid resolution is adequate.

Validation of numerical calculation

To validate the present numerical modelling, results of calculation are compared with Dally's measurements for cases 1-4 of tab. 1. Distribution of mean scalar mixture fraction (ξ),

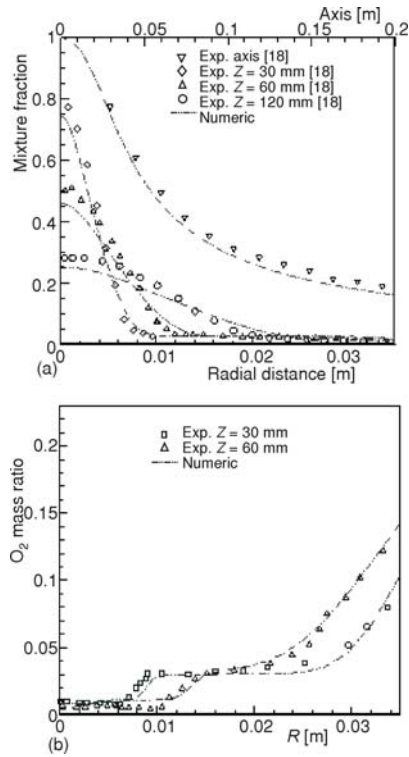


Figure 2. (a) Comparison mixture fraction profiles with experimental data at axial and radial directions for 9% O₂ (Case 1 in tab. 1), and (b) Experimental O₂ radial profiles vs. numerical results at Z = 30 mm and 60 mm for 3% O₂ (Case 2 in tab. 1)

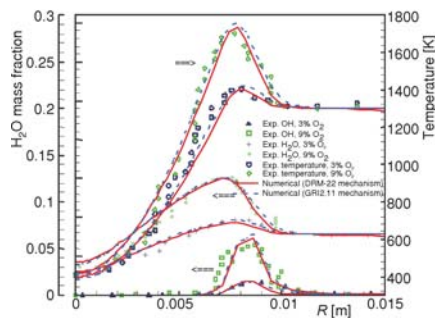


Figure 3. Experimental temperature, H₂O, and OH radial profiles vs. numerical results at Z = 30 mm for 3% O₂ and 9% O₂ and two chemical mechanisms of GRI2.11 and DRM-22 (Cases 1-4 in tab. 1)

computed using Bilger's formula [44], is compared with experiments in fig. 2(a). The equation of Bilger is:

$$\xi \equiv \frac{\frac{2Z_C}{W_C} + \frac{1}{2}\frac{Z_H}{W_H} + \frac{Z_{0,2} - Z_0}{W_0}}{\frac{2Z_{C,1}}{W_C} + \frac{1}{2}\frac{Z_{H,1}}{W_H} + \frac{Z_{0,2}}{W_0}} \quad (5)$$

where Z_j and W_j are the elemental mass fractions and atomic masses for the elements carbon, hydrogen and oxygen and the subscripts 1 and 2 refer to values in the fuel and hot co-flow diluted air streams, respectively. The figure shows mixture fraction profiles along the axis of jet and also radial profiles of mixture fraction at 30, 60, and 120 mm above the nozzle. It can be understood that the mixture fraction distribution is predicted satisfactory for 9% O₂ in hot co-flow. Using the all available measurements the radial distribution of O₂ mass fraction for 3% O₂ at Z = 30 and 60 mm are depicted in fig. 2(b). These results demonstrate a confidence in the predictions for the jet spreading and mixing.

Also radial distribution of temperature, OH, and H₂O mass fractions are compared with the experimental data for 3% and 9% O₂ in fig. 3. Based on the agreement between the numerical and experimental measurement for minor and main species and also temperature, it can be inferred that the chemical reactions and heat transfer phenomena are predicted with an acceptable level of accuracy.

To investigate the effect of the chemical mechanism on the results, a comparison of two mechanisms (*i. e.* DRM-22 and GRI2.11) are performed (fig. 3). There is a good agreement between the results of two chemical mechanisms especially near the flame axis where combustion occurs at the fuel rich side. As a result, the DRM-22 which has a lower cost of calculation is used in the continuation of modelling.

According to Dally *et al.* [18], the mixing with fresh air of tunnel air affects this flame above 100 mm from the nozzle. Therefore, the distance below 100 mm from the fuel jet nozzle is suitable for studying the MILD combustion regime in this experimental set-up.

Flame structure

To study the flame structure, the analysis is focused on the reaction zone and flow field. The distributions of important parameters such as mixture fraction, radial velocity, OH, HCO, CH₂O species, temperature, strain rate, Damkohler number, and flame entrainment and turbulence decay are considered. The velocity field, mixture fraction, strain rate, entrainment, and turbulence decay are useful for investigation of mixing and flow dynamics. Temperature field and species distribution help us to understand the reaction zone features in detail, also.

Case 4 in tab. 1 provides a good sample of MILD combustion, because it represents the main features of MILD regime such as the high level of dilution, as high as 3% O₂, high temperature preheating, and high Reynolds number which leads to high level of turbulence. To confirm the later selection, the temperature contours for four cases, including the Reynolds numbers of 5000 and 10000 and for two co-flow O₂ levels of 3 and 9%, are shown in fig. 4(a) and (b). Furthermore the radial profiles of temperature for four cases, which are depicted in fig. 4(a) and (b), at Z = 30 and 60 mm are compared in fig. 4(c). It is apparent from the figures that the temperature field is more uniform for 3% O₂ and Reynolds number of 10000 than the other cases. Increasing the O₂ level or decreasing of jet Reynolds number decreases this uniformity. However, O₂ level is more influential on temperature uniformity than the Reynolds number is.

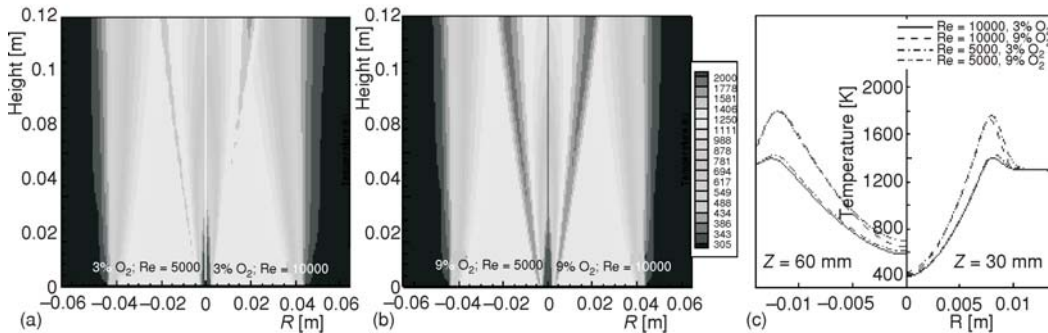


Figure 4. (a) Contours of temperature for 3% O₂ and two Reynolds numbers of 5000 and 10000 (Cases 4 and 7 in tab. 1), (b) Contours of temperature for 9% O₂ and two Reynolds numbers of 5000 and 10000 (Cases 3 and 6 in tab. 1), (c) Radial temperature profiles at Z = 30 mm and 60 mm for part a and b

In fig. 5(a), contours of CH₂O and OH are shown with HCO contours imposed on them. The hydroxyl (OH) can be used as flame marker and the formaldehyde (CH₂O) intermediate species is an ignition marker [23, 24]. Formaldehyde is the first-step intermediate products of fuel decomposition [23]. Najm *et al.* [45] suggested that the product of OH and CH₂O are an indicator of the formyl HCO radical, which is closely related to the heat release rate.

It can be seen that the OH species is concentrated in outer border of CH₂O contours and the CH₂O radical is present inside the diffusion layer. The CH₂O contour has a lower gradient far from the nozzle. It is referred to extended reaction zone at down stream, especially at Z < 100 mm, the range that is considered in this study. Furthermore, the concentrated spots of CH₂O at upstream show that the local powerful ignition occurs at diffusion layer.

Figure 5(a) shows that the contours of OH and HCO are discontinuous and there is a delay between them, *i. e.* the OH concentration decreases whenever the HCO concentration increases. The discontinuity in HCO, OH, and also CH₂O at reaction zone can be attributed to local extinction in reaction zone and shear layer. This flame structure is reported by Afarin *et al.*

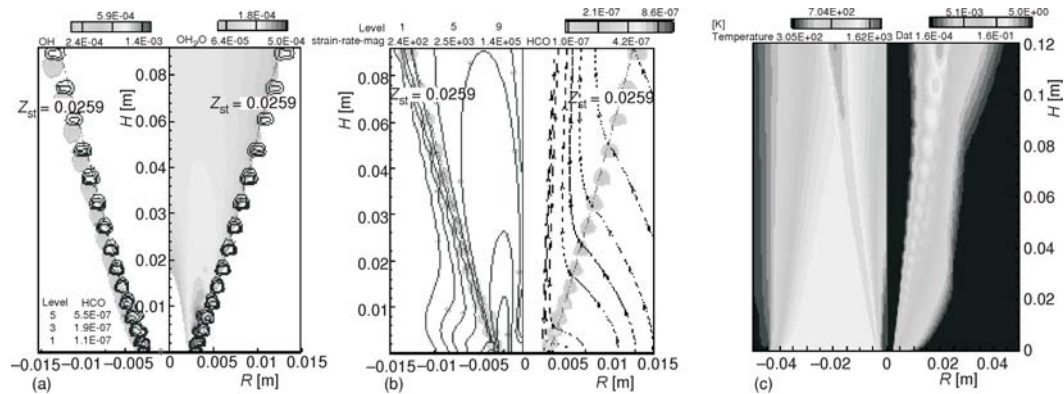


Figure 5. (a) Contours of CH₂O, OH, and HCO for 3% O₂, (b) Contours of HCO and strain rate and stream line for 3% O₂, (c) Contours of Temperature and Damkohler number for 3% O₂ and Re = 10000 (Case 4 in tab. 1)

[46] in which JHC burner is modelled using the large eddy simulation scheme. Furthermore, experimental results of Medwell *et al.* [23] on JHC burner, shows the existence of local discontinuity in CH₂O contours. Katsuki *et al.* [3] reported that such extinction is necessary for sustaining the MILD combustion regime in furnace environment. This idea could be used to explain that how the hot co-flow oxidizer penetrate into the jet and leads to expansion of the reaction zone in MILD regime. The stream lines, in fig. 5(b), illustrate that hot oxidizer flow deflects toward the reaction zone and this deflection decreases with distance from the nozzle. Furthermore, the above discussion, about minor species distribution, shows that the detail mechanism is essential for modelling of MILD regime and overall ordinary mechanism could provide wrong results. This has also been mentioned by Tsuji *et al.* [47]. The position of stoichiometric mixture fraction ($Mf_{st} = 0.0259$) is indicated in fig. 5(a) and (b) with width dash-dot-dot line. Contours of OH are intensified at air side of stoichiometric mixture fraction contour and contours of CH₂O at fuel sides', although contour of HCO has high intensity around stoichiometric mixture location. The contour of stoichiometric mixture fraction illustrates how the reaction zone does not occur exactly at stoichiometric mixture in this regime. The contours of temperature and Damkohler number are shown in fig. 5(c). The continuous temperature field and low increase of temperature in reaction zone are obvious. On the other hand, the Damkohler contour shows that the reactions are very slow in comparison with ordinary combustion. Also, Damkohler number increases by moving away from the nozzle. Specially at $Z > 100$ mm, the large Damkohler number demonstrates the MILD regime is transitioning to a diffusion flame due to the increase of reaction rates due to mixing with wind tunnel fresh air. This observation is consistent with the appropriate region as mentioned by Dally *et al.* [18] for study of MILD combustion.

Another important result of Damkohler number contour is the necessity of using slow burning theories in modelling of MILD combustion which is also mentioned before [47]. The strain rate contours in fig. 5(b), which is imposed on HCO contours, illustrates that the lower limit of strain rate in reaction zone is around 200 1/s. This limit changes from <5000 1/s to about 200 1/s by moving away from the nozzle.

For more detail, the radial profiles of radial velocity, temperature and strain rate at $Z = 30$ and 60 mm for 3% O₂ are depicted in fig. 6(a). Also, the stoichiometric mixture position is identified for $Z = 30$ and 60 mm in the figure. The figure shows that firstly, the reaction zone disappears at a strain rate below approximately 200 1/s. Second, the maximum reaction rate position is in the

fuel lean region. Third, the radial velocity distribution shows a minimum at stoichiometric location. That indicates that the turning point of radial velocity profiles occurs at the position of stoichiometric mixture, and it is due aerodynamic of the jet. Fourth, the mixing rate and the velocity gradients decrease with the distance from the nozzle. Fifth, the maximum flame temperature at $Z = 30$ and 60 mm are approximately the same, which means that the rates of heat release at these locations are similar.

Figure 6(b) is depicted for 23% O_2 , which is not under MILD conditions, (case 5 in tab. 1). Comparing fig. 6(a) and (b) shows that the maximums of temperature and radial velocity, and strain rate in hot air side decrease under the MILD condition. That means that velocity field, like temperature field, is much more uniform under this condition. This is due to a lower heat release rate and density gradient inside the extended reaction zone under high diluted combustion conditions.

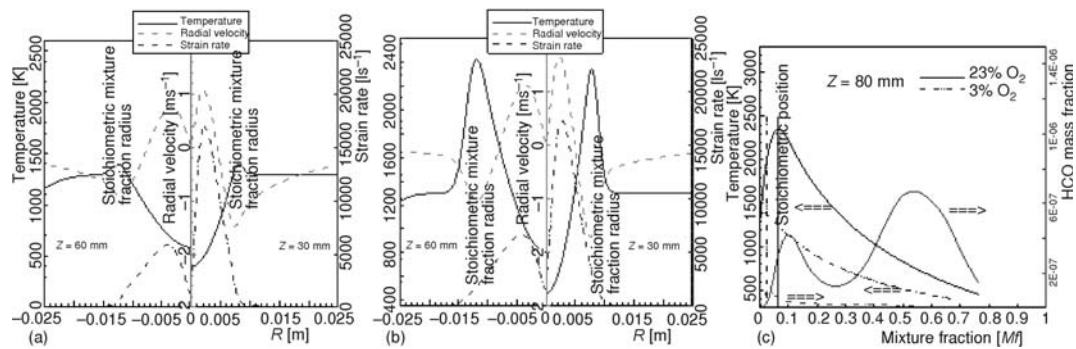


Figure 6. Radial distribution of temperature, strain rate, and radial velocity at $Z = 30$ and 60 mm for $Re = 10000$ and (a) 3% O_2 (Case 4 in tab. 1), (b) 23% O_2 (Case 5 in tab. 1), (c) Comparison of temperature and HCO profiles at mixture fraction domain for 3 and 23% O_2 at $Z = 30$ mm

It is worthwhile noticing the distributions of Formyl radical and temperature in mixture fraction domain for 3 and 23% O_2 in fig. 6(c). The temperature profiles illustrate that starting from 305 K at $Mf = 0$, the temperature increases up to the maximum value at $Mf_{st} = 0.0639$ in the case of 23% O_2 and $Mf > Mf_{st}$ ($Mf_{st} = 0.0259$) in the case of 3% O_2 . A decrease in stoichiometric mixture fraction from 0.0639 to 0.0259, by reducing the O_2 concentration from 23 to 3% O_2 , indicates the extension of reaction zone toward the air side (*i. e.* larger reaction zone). The related HCO profiles, in the same figure with red and width lines, show that the heat release is more uniform at lower O_2 levels and the second peak of HCO profile disappears for 3% O_2 . Analyzing the structure of reactive zone by Joannon *et al.* [48] shows that the pyrolysis region in the heat releases profiles disappear in MILD regime and moreover the maximum of heat release is not correlated with the stoichiometric mixture fraction. De-Joannon *et al.* [48] used a configuration of opposed jets of hot air vs. cold fuel/diluent mixture to study MILD combustion structure. It is worthwhile to notice that both results of Joannon, in a counter flow configuration, and present work, in a co-flow burner, illustrates some typical characteristics of standard diffusion flames are no longer present in MILD combustion regime.

Effect of co-flow oxygen content on flame structure

To study the effect of co-flow O_2 level on the flame structure, the radial profiles of flame parameters at $Z = 30$ for two different O_2 levels of 3 and 9% are presented in fig. 7. The mixture

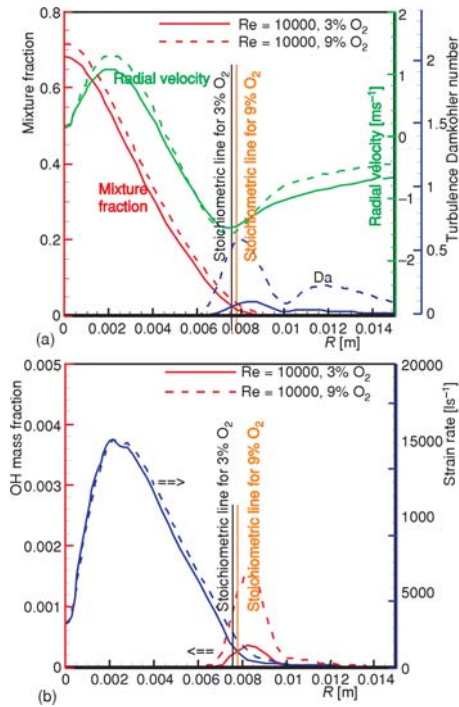


Figure 7. (a) Radial distribution of mixture fraction, Damkohler number, and radial velocity (b) Radial distribution of OH and strain rate (at $Z = 30$ mm for 3 and 9%O₂)

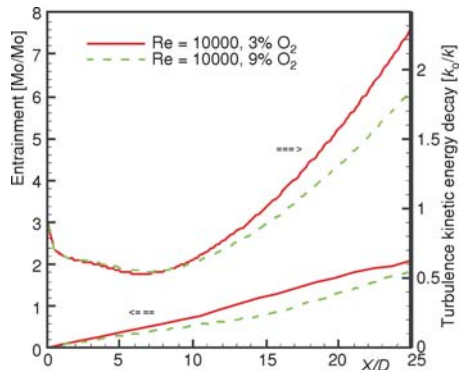


Figure 8. Flame entrainment and turbulence decay along the flame axis for Reynolds number of 10000 and two O₂ mass fraction of 3 and 9% O₂ (Cases 3 and 4 in tab. 1)

pation increases at lower O₂ concentration and under MILD conditions. This may be due to the smaller reaction zone and, consequently, less uniform heat release of higher O₂ levels. The expansion of fluid due to heat release reduces the vorticity and destroys the local vortex tubes [31].

fraction, radial velocity and Damkohler number are depicted in fig. 7(a). Furthermore, the OH and strain rate profiles are illustrated in fig. 7(b).

It can be seen that the increase of O₂ leads to an increase in radial velocity, Damkohler number, mixture fraction, OH mass fraction, and the strain rate. Damkohler number and OH increment illustrate that the rate of reactions have increased for higher O₂ level, which is predictable. The increase of radial velocity and strain rate reveal that the rate of mixing in reaction zone has increased by O₂ addition. It could be due to increase of temperature gradient and consequently density gradient as a result of higher heat release rate. The shift in the stoichiometric position outward the flame axis, indicates that there has been a decline in the thickness of diffusion layer. On the other hand, the higher value of mixture fraction inside the jet reveals lower presence of oxidizer molecules. That means that at lower O₂ level, the oxidizer has a higher penetration depth into the jet. This could be due to a weaker reaction intensity, which lets oxidizer pass through the reaction zone without reacting, and also larger and more uniform reaction zone.

Also, the position of maximum OH contour is closer to stoichiometric mixture location at higher O₂ concentration. That means the reaction zone is moving toward the stoichiometric region by increase of O₂ concentration in the hot air.

For more detail, the flame entrainment profiles for 3% and 9% O₂ are illustrated in figure 8. It can be understood that the flame entrainment increases by decreasing of O₂ concentration at the air side. This is in consistency with the discussion about the mixture fraction variations. This phenomenon is reported by Yang *et al.* [21]. He ascribed it to a decrease in reaction rates and more uniform heat release rate. To study that in more detail, the ratio of the turbulent kinetic energy at the nozzle inlet (k_o) to the turbulent kinetic energy along the flame axis (k) is also presented in fig. 8. That shows the turbulence kinetic energy decay at the centreline of the jet decreases by the increasing of O₂ concentration. In other words, the turbulence kinetic energy dissipation increases at lower O₂ concentration and under MILD conditions.

That is, the combustion dampens turbulence eddies and laminarizes the flow. The laminarizing of flow occurs over a larger zone at lower O_2 levels. Therefore, the mixing rate due to turbulence might not be so influential on the reduction of the flame entrainment at higher O_2 levels for present set-up and other mechanism of mixing, the molecular diffusion, may be more influential than the turbulence mixing. The importance of molecular diffusion in MILD regime was mentioned by other papers [16, 17, 19, 28].

Effect of Jet Reynolds number on flame structure

Effect of jet Reynolds number on the flame structure is studied in figs. 9 and 10. Figures 9(a) and (b) show that the radial velocity and strain rate decrease by reduction of jet Reynolds number from 10000 to 5000. Also, the mixture fraction, in regions near the stoichiometric zone, has a reduction. These imply that the rate of mixing and mixing intensity in the diffusion layer has decreased by jet Reynolds number reduction. Furthermore, the position of stoichiometric zone moves toward the flame axis by increasing the jet Reynolds. That means the mixing in the diffusion layer is such high as the stoichiometric condition occurs at a smaller radius for higher Reynolds numbers. The increase in OH mass fraction, by increase in Reynolds, reveals that the rate of reactions has increased although the Damkohler number has decreased.

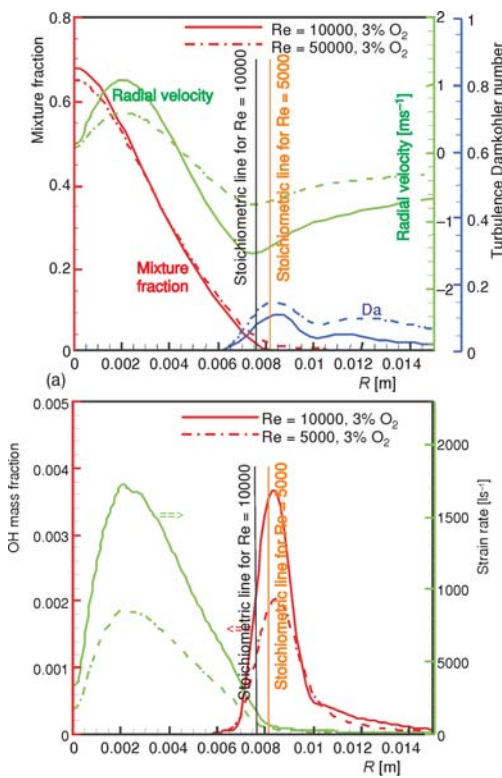


Figure 9 (a) Radial distribution of mixture fraction, Damkohler number, and radial velocity
(b) Radial distribution of OH and strain rate (at $Z = 30$ mm for 3% O_2 and $Re = 5000$ and 10000) (Cases 4 and 7 in tab. 1)

This perhaps is due to the effect of higher turbulence level at Reynolds number of 10000 in comparison with 5000.

The entrainment and turbulence decay, along the flame axis, are also depicted in fig. 10, for two Reynolds numbers of 10000 and 5000. That shows that although the flame entrainment decreases by increase of jet Reynolds number, the turbulence decay does not change considerably. Higher flame entrainment, at low Reynolds number, can be due to wider reaction zone as which discussed before. On the other hand, the similar turbulence decay for two

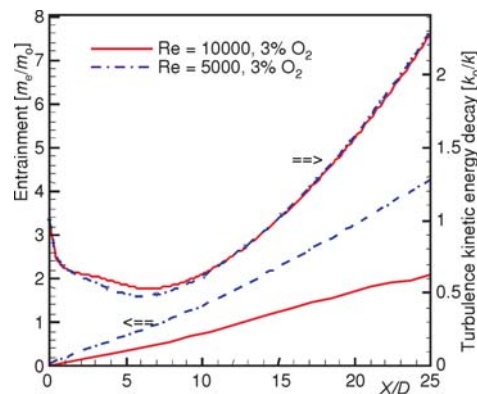


Figure 10. Flame entrainment and turbulence energy decay along the flame axis for two Reynolds numbers of 5000 and 10000 and O_2 mass fraction of 3% O_2 (Cases 4 and 7 in tab. 1)

Reynolds numbers shows that the turbulence level at $Re=10000$ is higher than that at $Re = 5000$ and this could be important in increment of the flame entrainment by increase in Reynolds number at constant O_2 level. This contradictory leads us to conclude that other mechanism of transition like molecular diffusion could be important.

Comparing fig. 8 with fig. 10 illustrates two important features of fuel jet discharged into a hot and diluted atmosphere. First, the turbulence decay is not sensitive to inlet jet Reynolds number, however it changes by variation of O_2 level. Second, the flame entrainment is more sensitive to jet Reynolds number than to the O_2 level.

Conclusions

The flame structure in MILD combustion regime is studied numerically. The study is considered by modelling of a fuel jet issuing into a hot and much diluted atmosphere using RANS equations and details chemical mechanisms. The reaction zone, mixing, flame entrainment, turbulence decay, and species concentrations are investigated. Results of calculation and experiment are compared and there is a good agreement between them.

Results show that the position of the maximum reaction rate occurs on the fuel lean side and the radial velocity distribution is minimum at stoichiometric location. Also, the mixing rate, and the velocity gradients decrease with the distance from the nozzle. Focusing on the reaction zone illustrate that CH_2O radical is present inside the jet which is fuel rich region. On the other hand, the contours of OH and HCO are discontinuous and this discontinuity in the reaction zone can be referred to local extinction in the reaction zone.

A decrease in O_2 concentration in hot co-flow at constant jet Reynolds number leads to decrease in rate of reactions, OH concentration, radial velocity, Damkohler number, mixture fraction, and strain rate in the jet flame. In other word, the rate of reaction and rate of mixing decrease and reaction zone area and its uniformity increase by reduction of O_2 level. Also, the reaction zone is moving toward the stoichiometric region by the increase in O_2 concentration of hot air. On the other hand, increase in jet Reynolds number increases the mixing rate and rate of reactions greatly. Furthermore, the position of stoichiometric zone moves toward the flame axis by increasing the jet Reynolds.

The flame entrainment decreases by the increase in jet Reynolds or O_2 concentration in co-flow air. Also, the turbulence kinetic energy decay at centreline of the jet decreases by the increase in O_2 concentration at hot co-flow but its variation by changing the jet Reynolds number is marginal. As a whole, a fuel jet emerging to hot and very lean atmosphere, which emulates MILD condition, illustrates higher flame entrainment, higher turbulence decay, lower velocity and temperature gradient, and larger broken reaction zone area in comparison with jet flames under higher O_2 concentration and the same preheating condition.

Nomenclature

c_r	– chemical reaction rate constant (Inverse of chemical reactions time scale), [s^{-1}]	v	– radial velocity, [ms^{-1}]
Da_T	– turbulent Damkohler number, [-]	z	– axial distance from fuel nozzle inlet, [mm]
k	– local turbulent kinetic energy, [m^2s^{-2}]	<i>Greek symbols</i>	
m_e	– mass flow rate through the cross-section of the flame, [kgs^{-1}]	ε	– local dissipation rate of turbulent kinetic energy, [m^2s^{-3}]
m_o	– initial jet mass flow rate, [kgs^{-1}]	ν	– kinematic viscosity, [m^2s^{-1}]
Re	– Reynolds number ($= \rho u D / \mu$), [-]	ρ	– density, [kgm^{-3}]
R_{ent}	– flame entrainment ($= m_e / m_o$), [-]	ξ	– mean scalar mixture fraction, [-]
S	– strain rate, [s^{-1}]		
u	– axial velocity, [ms^{-1}]		

References

- [1] Cavaliere, A., Joannon, M. D., MILD Combustion, *Prog. Energy Combust. Sci.*, 30 (2004), pp. 329-366
- [2] Niioka, T., Fundamentals and Applications of High-Temperature Air Combustion, 5th ASME/ JSME Jt. Therm. Conf. (AJTE) 99- 6301, San Diego, Cal., USA, 1999, pp.1-6
- [3] Katsuki, M., Hasegawa, T., The Science and Technology of Combustion in Highly Preheated Air, *Proc. Combust. Ins.*, 27 (1998), pp. 3135-3146
- [4] Niioka, T., Impact of Knowledge Gained from the HiCOT Project on Development of Combustors, *Proceedings*, 5th Asia-Pacific Conf. Combust., Adelaide, Australia, 2005, pp. 1-4
- [5] Wunning, J. G., Flameless Combustion in Thermal Process Technology, *Proceedings*, 2th Int. Semin. on High Temperature Air Combust., Stockholm, Sweden, 2000
- [6] Ito, Y., et al., Combustion Characteristics of Low Calorific Value Gas with High Temperature and Low-Oxygen Concentration Air, *Proceedings*, 5th HiTAC Gasif. Conf., Yokohama, Japan, 2002
- [7] Mortberg, M., et al., Experimental Investigation of Flow Phenomena of a Single Fuel Jet in Cross-Flow during Highly Preheated Air Combustion Conditions, *J. Eng. Gas Turbines Power*, 129 (2007), pp. 556-564
- [8] Gupta, A. K., Li, Z., Effect of Fuel Property on the Structure of Highly Preheated Air Flames, *Proceedings*, Int. Jt. Power Gener. Conf., Palo Alto, Cal., USA, ASME EC; Vol. 5, 1997, pp. 247-258
- [9] Gupta, A. K., Flame Length and Ignition Delay during the Combustion of Acetylene in High Temperature Air, *Proceedings*, 5th HiTAC Gasifi. Conf., Yokohama, Japan, 2002
- [10] Fuse, R., et al., NO_x Emission from High-Temperature Air/ Methane Counterflow Diffusion Flame, *Int. J. Therm. Sci.*, 41 (2002), pp. 693-698
- [11] Hasegawa, T., et al., High Temperature Air Combustion Contributing to Energy Saving and Pollutant Reduction in Industrial Furnace, *Proceedings*, Int. Jt. Power Gener. Conf., Palo Alto, Cal., USA, ASME; 1997, pp. 259-266
- [12] Guo, H., et al., Junichi Sato, Numerical Study of NO_x Emission in High Temperature Air Combustion, *JSME Int. J.*, B41 (1998), 2, pp. 331-337
- [13] Hasegawa, T., et al., Development of Advanced Industrial Furnace Using Highly Preheated Air Combustion, *J. Propul. Power*, 18 (2002), 2, pp. 233-239
- [14] Plessing, T., et al., Laser Optical Investigation of Highly Preheated Combustion with Strong Exhaust Gas Recirculation, *Proc. Combust. Ins.*, 27 (1998), pp. 3197-3204
- [15] Mortberg, M., et al., Combustion of Normal and Low Calorific Fuels in High Temperature and Oxygen Deficient Environment, *Combust. Sci. Tech.*, 178 (2006), pp. 1345-1372
- [16] Christo, F. C., Dally, B. B., Modeling Turbulent Reacting Jets Issuing into a Hot and Diluted Co-flow, *Combust. Flame*, 142 (2005), pp. 117-129
- [17] Kim, S. H., et al., Conditional Moment Closure Modelling of Turbulent Non-Premixed Combustion in Diluted Hot Co-Flow, *Proc. Combust. Ins.*, 30 (2005), pp. 751-757
- [18] Dally, B. B., et al., Structure of Turbulent Non-Premixed Jet Flames in a Diluted Hot Co-flow, *Proc. Combust. Ins.*, 29 (2002), 1, pp. 1147-1154
- [19] Mardani, A., Tabejamaat, S., Numerical Study of Influence of Molecular Diffusion in the MILD Combustion Regime, *Combust. Theory and Modelling*, 14 (2010), pp. 747-774
- [20] Kobayashi, H., et al., Effects of Turbulence on Flame Structure and NO_x Emission of Turbulent Jet Non-Premixed Flames in HiTAC, *JSME Int. J.*, 48B (2005), 2, pp. 286-292
- [21] Yang, W., Blasiak, W., Flame Entrainments Induced by a Turbulent Reacting Jet Using High-Temperature and Oxygen-Deficient Oxidizers, *Energy Fuels*, 19 (2005), pp. 1473-1483
- [22] Oldenhof, E., et al., Role of Entrainment in the Stabilisation of Jet-In-Hot-Coflow Flames, *Combust. Flame*, 158 (2011), pp.1553
- [23] Medwell, P. R., et al., Simultaneous Imaging of OH, Formaldehyde, and Temperature of Turbulent Non-Premixed Jet Flames in a Heated and Diluted Co-flow, *Combust. Flame*, 148 (2006), pp. 48-61
- [24] Parente, A., et al., Effect of the Combustion Model and Kinetic Mechanism on the MILD Combustion in an Industrial Burner Fed with Hydrogen Enriched Fuels, *Int. J. Hydrogen Energy*, 33 (2008), pp. 7553-7564
- [25] Gupta, A. K., High Temperature Air Combustion (HiTAC) Technology, *Proceedings*, 18th Int. Symp. Combust. Processes, Ustron, Poland, 2003
- [26] Weber, R., et al., On Emerging Furnace Design Methodology That Provides Substantial Energy Savings and Drastic Reductions, *J. Inst. Energy*, 72 (1999), 492, pp. 77-83

- [27] Weber, R., et al., On Emerging Furnace Design Methodology that Provides Substantial Energy Savings and Drastic Reductions in CO₂, CO and NO_x Emissions, *Proceedings*, 2th Int. Seminar High Temperature Combust. Ind. Furn., Stockholm, Sweden, 2000
- [28] Mardani, A., Tabejamaat, S., Effect of Hydrogen on Hydrogene-Methane Turbulent Non-Premixed Flame under MILD Condition, *Int. J. Hydrogen Energy*, 35 (2010) pp. 11324-11331
- [29] Mardani, A., et al., Numerical Study of the Effect of Turbulence on Rate of Reactions in the MILD Combustion Regime, *Combust. Theory and Modelling*, 15 (2011), 6, pp.753
- [30] Mardani, A., Tabejamaat, S., NO_x Formation in H₂-CH₄ Blended Flame under MILD Condition, *Combust. Sci. Technol.*, 184 (2012), 7-8, pp. 995-1100
- [31] Kuo, K. K., Principle of Combustion, John Wiley & Sons, Inc., New York, USA, 1986, chapters 3&4 & p. 430
- [32] Rahman, M.M., et al., Modified Simple Formulation on a Collocated Grid with an Assessment of the Simplified Quick Scheme, *Numer. Heat Trans.*, B30 (1996), 3, pp. 291-314
- [33] Frassoldati, A., et al., Kinetic and Fluid Dynamics Modeling of Methane/Hydrogen Jet Flames in Diluted Coflow, *Appl. Therm. Eng.*, 30 (2010), pp. 376-383
- [34] Maruta, K., et al., Reaction Zone Structure in Flameless Combustion, *Proc. Combust. Inst.*, 28 (2000), 2, pp. 2117-2123
- [35] Gran, I. R., Magnussen, B. F., A Numerical Study of a Bluff-Body Stabilized Diffusion Flame. Part 2. Influence of Combustion Modeling and Finite-Rate Chemistry, *Combust. Sci. Technol.*, 119 (1996), pp. 191-217
- [36] Yang, W., et al., Mathematics Modelling for High Temperature Air Combustion (HiTAC), Summary Final Report, Royal Institute of Technology (KTH), 2003
- [37] De, A., et al., Numerical Simulation of Delft-Jet-in-Hot-Coflow (DJHC) Flames Using the Eddy Dissipation Concept Model for Turbulence-Chemistry Interaction, *Flow Turbulence Combust.*, 87 (2011), 4, pp. 537-567
- [38] Kazakov, A., Frenklach, M., Reduced Reaction Sets Based on GRIMech1.2., Available at <<http://www.me.berkeley.edu/drm/>>
- [39] Frenklach, M., et al., (1994) GRI-1.2., Available at http://www.me.berkeley.edu/gri_mech/
- [40] Bowman, C. T., et al., GRI-2.11., Available at <http://www.me.berkeley.edu/gri_mech/>
- [41] Warnatz, J., et al., *Combustion*, Springer, Germany, 1996, p. 186
- [42] Blasiak, W., et al., Physical Properties of a High Temperature Flame of Air and LPG on a Regenerative Burner, *Combust. Flame*, 136 (2004), pp. 567-569
- [43] Yang, W., Blasiak, W., Numerical Study of Fuel Temperature Influence on Single Gas Jet Combustion in Highly Preheated and Oxygen Deficient Air, *Energy*, 30 (2005), 2-4, pp. 385-398
- [44] Bilger, R. W., et al., On Reduced Mechanisms for Methane-Air Combustion in Non-Premixed Flames, *Combust. Flame*, 80 (1990), pp. 135-149
- [45] Najm, H. N., et al., On the Adequacy of Certain Experimental Observables as Measurements of Flame Burning Rate, *Combust. Flame*, 113 (1998), pp. 312-332.
- [46] Afarin, Y., et al., Large Eddy Simulation Study of H₂/CH₄ Flame Structure at MILD Condition, MCS 7, Chia Laguna, Cagliari, Sardinia, Italy, 2011
- [47] Tsuji, H., et al., High Temperature Air Combustion: From Energy Conservation to Pollution Reduction, CRC Press, Boca Raton, Fla., USA, 2003
- [48] De Joannon, M., et al., Numerical Study of MILD Combustion in Hot Diluted Diffusion Ignition (HDDI) Regime, *Proc. Combust. Ins.*, 32 (2009), 2, pp. 3147-3154